ARTICLE

Improvement in liquid absorption of open-cell polymeric foam by plasma treatment for food packaging applications

Alaa Alaizoki[1] ● | Christopher Phillips[1] ● | David Parker[2] | Craig Hardwick[2] |
James McGettrick[1] ● | Davide Deganello[1] ●

[1]Faculty of Science and Engineering, Swansea University, Swansea, UK

[2]Klockner Pentaplast, Featherstone, West Yorkshire, UK

Correspondence
Alaa Alaizoki and Davide Deganello, Faculty of Science and Engineering, Swansea University, Swansea SA1 8EN, UK.
Email: d.deganello@swansea.ac.uk (D. D.) and 972353@swansea.ac.uk (A. A.)

Abstract

Free-moving meat exudate in plastic packaging is perceived as unhygienic and unattractive by consumers. It facilitates the deterioration of meat quality and safety, increasing meat waste and loss. This work discusses an innovative approach in scavenging meat exudate within commercial plastic packaging. This involves improving the liquid absorption capabilities of open-cell polystyrene (PS) foam through the application of oxygen plasma treatment rather than chemical wetting agents. The excited plasma species diffuse into the porous foam structure introducing polar oxygen groups onto the pore walls and improves their surface hydrophilicity. Hence, the foam pores, with enhanced wettability towards water-based liquids, are proposed to have a larger sucking capillary pressure thus increasing the absorption capacity of the porous PS foam. The specific liquid absorption capacity of PS foam sheets (thickness: 5 mm) increased from 1.09 g g^{-1} (grams of exudate simulant liquid absorbed per gram of PS foam) to 8.78 g g^{-1} as a result of plasma treatment; an eightfold increase in liquid capacity (g g^{-1}) that persisted even 60 days post treatment. This study demonstrates the practicality of using plasma treatment as a non-chemical and efficient technology in scavenging meat and food exudates in plastic packaging.

KEYWORDS

foams, packaging, polystyrene

1 | INTRODUCTION

Food freshness, safety, and shelf life are crucially dependent on food packaging. The packaging provides a protection to the contained food from various physical and chemical contaminants, and it inhibits the proliferation of spoilage and pathogenic bacteria.[1–3] The development of food packaging functionalities is gaining more interest

in light of growing demand for safer, healthier and longer shelf-life food.[3] Furthermore, supply chains will be required to secure ~70% more food in 2050 as the global population is estimated to exceed 9 billion.[4] This can threaten global food security, particularly since one third of globally produced food is wasted every year.[5] Therefore, the packaging industry has been driven to develop functionalized packaging solutions to reduce food waste

by addressing current challenges of packaged food products, such as exuded liquid from food.[1] Fresh meat, fish, and poultry are perishable products, which tend to excrete liquid (exudate) in the packaging during their shelf life.[1,6] Meat exudate is an aqueous liquid containing soluble sarcoplasmic proteins with a mixture of amino acids and enzymes.[7] It is formed and purged as the muscle proteins denature during the post-mortem process. This exudate loss reaches 1–3wt% of a fresh meat piece and it can increase for meat that has been processed, chopped or frozen.[8,9] Meat quality and safety are adversely affected by the exudate leading to limited shelf life of the packaged meat products. This is attributed to the increased water activity, and thus greater proliferation of microorganisms responsible for meat spoilage.[1] Consequently, the efforts to meet the increased meat demand will be undermined with more than 20% of meat supply wasted.[10] The free-moving exudate in the meat packaging also provides an unsightly appearance to consumers and it can leak from the packaged product.[11] Therefore, it is of great importance to develop a packaging solution to isolate the released exudate from the packaged meat products.

Fresh meat products are normally packaged in polymeric trays and sealed with thin flexible films.[11] Isolation of the meat exudate in these trays has thus far been addressed by different packaging solutions, such as addition of an absorbent pad,[12] and incorporation of meat trays with liquid-holding microwells.[13] However, these current solutions provide limited isolation capacity for meat exudate. The employing of absorbent pads also introduces additional cost and processing complexity.[14,15] A meat tray made of polymeric open-cell foam is an alternative packaging solution acting as both the container and soak-away for the meat exudate,[16,17] as shown in Figure 1. This absorbent
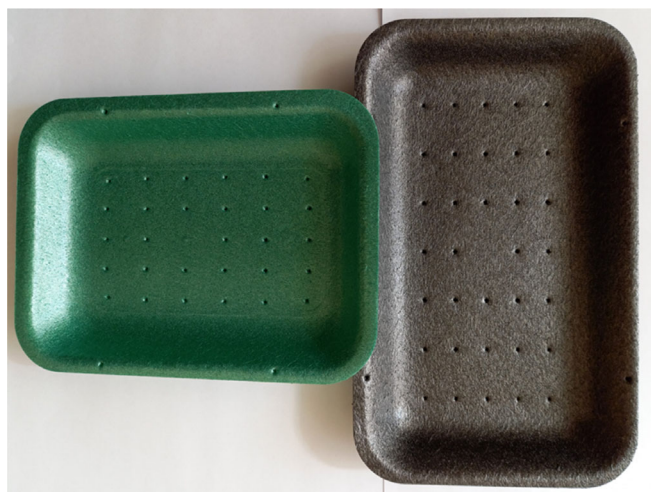

FIGURE 1 Open-cell polystyrene foam trays (trays source: Klockner Pentaplast Group) [Color figure can be viewed at wileyonlinelibrary.com]

tray has an interconnected porous structure and draws the meat exudate into the foam pores through perforations made in the tray skin.[17] The liquid absorbency of polymeric foams is attributed to their porosity and pore interconnectivity, which ensure a network of interconnected voids accessible to the wicked liquids.[18,19] However, a limitation of this effect is that the liquid absorption is only initiated as the liquid wets the pore surfaces. This characteristic of the porous material is a crucial property for liquid absorption, and it involves the liquid penetration under the influence of capillary pressure (P_c), as described by Young–Laplace Equation[20,21]:

$$P_c = \frac{2\gamma \cos\theta}{r},\qquad(1)$$

where γ is the liquid surface tension (N m^{-1}), θ is the liquid contact angle on pore surface (°), r is the radius of the foam pore (m). Therefore, any increase in wettability of the foam pores through reduction of the contact angle improves the sucking capillary pressure and increases the absorption capacity of the aqueous liquids.[19,22] A limitation of this mechanism is due to the inherently hydrophobic properties of foam packaging materials, such as polystyrene (PS) and polypropylene (PP), which restrict the penetration of hydrophilic liquids into the foam matrix.[23,24] Therefore, a wetting agent can be added to the foam trays to facilitate the liquid absorption.[25,26] This includes the addition of surfactants such as alkyl sulphonates, which enhance the wettability of foam pores with respect to the aqueous liquids.[26] For example, water uptake of poly-(lactide) (PLA) foam was reported to reach 27% (based on the pore volume) after adding poloxamer surfactant, while the foam did not absorb water before adding the surfactant.[27] However, there are concerns about these chemicals entering the food chain, leading to bioaccumulation and their potential toxic effects on the environment at high concentrations.[28,29]

As an alternative to the use of surfactants, the inherent surface wettability of polymeric materials can be altered by various surface modification treatments.[30] Plasma treatment is one of the most efficient techniques in increasing the wettability of polymeric surfaces.[2] Plasma is generated by ionizing gas molecules such as oxygen or air under the influence of an electric field. It is a glow of highly reactive gas molecules and particles with UV irradiation.[31,32] These excited species can functionalize the polymer surfaces with oxygen groups such COOH and C—OH inducing an increase in the surface polarity and wettability.[32] Plasma treatment is economical, eco-friendly, consistent, and capable of modifying the surface of complex objects.[33–35] Atmospheric plasma is

also efficient and practical for the packaging industry as it is suitable for in-line integration ensuring continuous processing.[36] Plasma treatment has been demonstrated to enhance liquid absorption by improving wettability for different textile materials, such as nonwoven polymeric substrates and silk fabrics.[37–39] Plasma technology is already applied to current food packaging to enhance the adhesion, printability, and film barrier properties.[2] The authors recently demonstrated the use of plasma in food packaging by locally functionalized recesses in solid plastic packaging.[40] However, there is no previous work on application of plasma treatment for liquid management in foam packaging.

This work therefore explores the use of plasma treatment on the porous structure of open-cell polymeric foams as a method of improving the wettability of their pore walls, and hence increasing their capacity for retaining liquids. It is proposed that this treatment may increase the sucking capillary pressure acting on the foam pores leading to improved liquid wicking and absorption. In this study, open-cell PS foam sheets are extruded and cut into cubic samples. Oxygen plasma is used to treat the foam samples and the impact of this treatment on their liquid absorption capacity is evaluated. Different test liquids are prepared to simulate meat exudate for the liquid absorption experiments. The liquid absorption capacity of the PS foam samples is compared before and after the plasma treatments. Surface characterization of the foam is performed in terms of wettability and chemical composition by water contact angle (WCA) and X-ray photoelectron spectroscopy (XPS) techniques respectively. The longevity of the plasma treatment is investigated by carrying out liquid absorption tests after different post-treatment times.

2 | EXPERIMENTAL SECTION

2.1 | Materials

Open-cell PS foam was supplied as plain sheets with thickness of 5 mm from large-scale industrial foam (Klockner Pentaplast Group). The foam sheet had impermeable skin on top and bottom sides, and it was cut into rectangle-shaped samples for surface characterization and absorption tests. Deionized (DI) water was used to prepare test liquids with different surface tension values (72.6, 52.3, 31.5 mN m^{-1}), to cover a range of wetting behaviors of meat exudate, by adding Triton X100 surfactant (Sigma Aldrich). Bovine serum albumin (BSA) (Sigma Aldrich) was used to prepare aqueous test liquid reflecting the presence of proteins in meat exudate. Red azorubine colorant-E122 (FastColours LLP) was added to stain the test liquids for absorption tests.

2.2 | Structural characterization of polystyrene foam materials

2.2.1 | Foam density and expansion ratio

Representative cubic samples were taken from PS foam by a sharp scalpel. The foam samples had dimensions ($L \times W \times T$: 20 mm × 20 mm × 5 mm) and were weighed on analytical scale (Model: A200S, Sartorius Analytic) with resolution of 0.0001 g. The density of PS foam was based on ratio of the mass of the foam samples to their geometric volumes as described in another work.[41] Expansion ratio (ψ) measurement was based on the ratio of solid PS polymer density (ρ_s) to the measured density of PS foam sample (ρ_f) as shown in Equation (2)[23]:

$$\psi = \frac{\rho_s}{\rho_f}, \tag{2}$$

ρ_s, ρ_f: kg m^{-3}.

The foam density and expansion ratio were average values of measurements carried out for six PS foam samples.

2.2.2 | Porosity and pore size distribution

The porosity (n) of PS foam represents the ratio of gas volume (V_{gas}) occupying pore spaces to the geometric volume of the foam sample (V_f). The volume of pore space was calculated by subtracting the volume of solid polymer (V_s) from the geometric volume of the foam sample (V_f) with dimensions ($L \times W \times T$: 20 mm × 20 mm × 5 mm). Therefore, the foam porosity was determined by compensating the volume with the corresponding mass and density as shown in Equation (3):

$$n = \frac{V_f - V_s}{V_f} = \frac{\frac{m_f}{\rho_f} - \frac{m_f}{\rho_s}}{\frac{m_f}{\rho_f}} = 1 - \frac{\rho_f}{\rho_s}, \tag{3}$$

where m_f (kg) is the mass of the foam sample, ρ_f (kg m^{-3}) is the density of the foam sample, ρ_s (kg m^{-3}) is the density of the solid polymer.[19]

The porosity measurements were repeated for six PS foam samples.

The pore structure and pore size distribution of PS foam was characterized by scanning electron microscope (SEM, Zeiss Evo-LS25). The cross-sections of intact foam samples were prepared for imaging by scoring the foam samples with a scalpel and immersing in liquid nitrogen (30 min). The scored samples were then fractured and sputtered with a layer of platinum coating (approximately

10 nm) using Agar High Resolution Coater (Model: 208HR, Agar Scientific) to reduce the charging effect during scanning. The sputter coating was performed with working pressure of 0.02 mbar and current of 80 mA. Two adjacent cross-section surfaces of six samples were then scanned and imaged by SEM operating at (15 kV) and within width of (2.287 mm). The SEM images were analyzed by ImageJ software (Version: 1.47v) to determine the pore size distribution. The pore size measurement was carried out by fitting a circle on each pore perimeter and measuring the corresponding diameter. The measured values of pore diameters were used to generate a histogram showing the distribution of pore sizes.[24]

2.2.3 | Open cell content

Open-cell content of PS foam was measured to evaluate the portion of interconnected cells in the foam samples. The open cells form the accessible volume of foam matrix where liquid can flow, while the remaining portion consists of closed compartments and pore walls. The content of open cells was based on the ratio of total open-cell volume to the geometric volume of the foam sample. This was measured by a gas pycnometer (ULTRAPYC 1200e—Quantachrome Instruments). The open cell content was calculated from the difference between the pycnometer volume and geometric volume of foam samples as given by the Equation (4):

$$\text{Open cell content \%} = \left[\frac{V_f - V_p}{V_f \times n}\right] \times 100. \quad (4)$$

The content of cell walls and closed cells was determined as shown in the Equations (5) and (6) respectively:

$$\text{Cell wall content \%} = \left[\frac{m_f}{\rho_s \times V_f}\right] \times 100, \quad (5)$$

$$\text{Closed cell content \%} = 100 - (\text{open cell content \%} + \text{cell wall content \%}), \quad (6)$$

where V_f (m^3) is geometric volume of foam sample, V_p (m^3) is pycnometer volume, n is porosity, m_f (kg) is mass of foam sample, ρ_s (kg m^{-3}) is density of solid PS polymer.

The measurements were carried out based on ASTM Standard D6226-10 as described in another work.[41]

2.3 | Oxygen plasma treatment of polystyrene foam

Samples for plasma treatment were taken from PS foam sheets of 5 mm thickness, with skin on the top and bottom faces of the sheet. Cut foam sections were treated with low-pressure plasma (Diener Electronic), with samples oriented to focus the plasma on the skin or edges as required. The plasma discharge was generated using supplied oxygen gas under an electric field (40 kHz). The loaded samples were outgassed as the unit chamber was pumped to low pressure (0.12 mbar). The O_2 plasma treatments were conducted for exposure time of 27 s at power of 240 W, with treatment duration based on preliminary experiments for achieving a target wettability (WCA: ~15°) on foam skin. The treated foam samples were then put in clean plastic containers to minimize any accidental contamination.[42]

2.4 | Surface characterization of the polystyrene foam

2.4.1 | Surface chemical composition by X-ray photoelectron spectroscopy analysis

The surface composition and functional groups of PS foam surface were analyzed by X-ray photoelectron spectroscopy provided with Axis supra system (Kratos Analytical Ltd). Survey scans were carried out to determine the surface elements on untreated and O_2 plasma-treated PS samples. The foam samples were irradiated at 1486.6 eV from an X-ray source of monochromatic Al Kα. The XPS scans were carried out at take-off angle of 90° and the resulting photoelectrons were received and analyzed by an encountering hemispherical analyzer. The surface charging was neutralized via the integral filament and magnetic lens system. The wide scan spectra were generated at pass energy of 160 eV and within a range of binding energy of 0–1400 eV. The high-resolution scans for C 1 s peaks were performed at pass energy of 20 eV. The peaks of all scan spectra were fitted on Shirley background and processed by CasaXPS software (Version 2.3.22PR1.0, Casa Software Ltd). Carbon peak components were deconvoluted and normalized with Gauss–Lorentz peak models to represent the different chemical groups in the carbon peak and calculate their concentrations. The surface chemical analysis was carried out for three PS foam samples.[43,44]

2.4.2 | Contact angle measurement

Static contact angles were measured on PS foam skin of untreated and plasma-treated samples using the sessile drop method. A micropipette was used to produce drops of DI water (3 μl) on the sample skin to evaluate the surface wettability. The measurements of the contact angles were carried out by goniometer (FTA1000c, First Ten Angstroms) and the resulting drop profiles were analyzed by FTA32 shape analyzer software. All contact angle measurements were conducted at a room temperature of $20 \pm 1°C$.[45]

2.4.3 | Water drop absorption test

DI water drops (10 μl) were placed on the cut sides of the foam samples with exposed porous structure (no skin) before and after plasma treatment. The time for the water drops to be fully wicked into the porous PS structure was measured by high-speed camera (Fastcam Mini, Model: UX100, Photron). The recorded wicking times were averaged for six water drops in different locations of the foam samples. A photograph was also taken for the water drops on the porous structure of the untreated and plasma-treated foam samples to compare their surface hydrophilicity.[46,47]

2.5 | Liquid absorption capacity

The absorption capacity of PS foam was determined for foam samples of dimensions ($L \times W \times T$: 40 mm $\times$ 10 mm $\times$ 5 mm). BSA 8wt% (γ: 52.0 mN m^{-1}), and DI water with added surfactant were used as test liquids of different surface tensions (γ: 72.6, 52.3, 31.5 mN m^{-1}). These cover a range of surface tensions of meat exudate that might be expected as well as extremes. The foam samples were treated with O$_2$ plasma for 27 s with samples oriented to focus the plasma on one cut side ($L \times T$). The absorption test was performed by freely placing the cross-sections ($L \times T$) of the untreated and plasma-treated samples on the test liquid within a plastic plate. The measurements of absorption capacity were repeated three times at room temperature of $20 \pm 1°C$, and estimated by the liquid weight in grams absorbed per gram of dry foam sample in equilibrium. The dry foam samples were weighed before the absorption test (W_d) and after their saturation with test liquid for 15 min (W_s). The foam samples were removed from the liquid for 30 s to allow any excess liquid to drain before weighing. The resulting absorption capacity (R) was given by Equation (7)[47,48]:

$$R = \frac{W_s - W_d}{W_d}. \tag{7}$$

2.6 | Aging effect

The changes in surface characteristics and absorption capacity due to aging phenomena were studied for plasma-treated PS foam after various storage times. All samples were stored in sealed plastic boxes at room temperature of $20 \pm 1°C$ as normal storage conditions after oxygen plasma treatment of 27 s. The surface wettability and chemical composition of the aged foam samples were characterized by WCA and XPS techniques respectively.[44] The absorption capacity (R) was measured for the foam samples with BSA 8wt% (γ: 52.0 mN m^{-1}). The surface wettability, chemical composition, and absorption capacity were determined with three repeats per measurement in different durations over 60 days.[43] For practicality of using PS foam as a soak-away in food packaging, the liquid absorption capacity was also estimated in kilograms of absorbed liquid per cubic meter of the PS foam.

3 | RESULTS

3.1 | Porous structure properties of polystyrene foam

Table 1 shows the material characteristics of PS foam samples. The PS foam had low density (41.61 kg m^{-3}) and large expansion ratio (25.24). The gaseous void content of the foam structure was represented by a porosity of 96%. This high porosity included closed and open cells, which are determined by the ratio of gaseous volume to the foam matrix volume. The open cells presented the interconnected foam pores showing high connectivity and open-cell content (90.91%).[18] The closed-cell content was only (4.24%) and solid PS material was estimated by

TABLE 1 Material properties of open-cell polystyrene foam

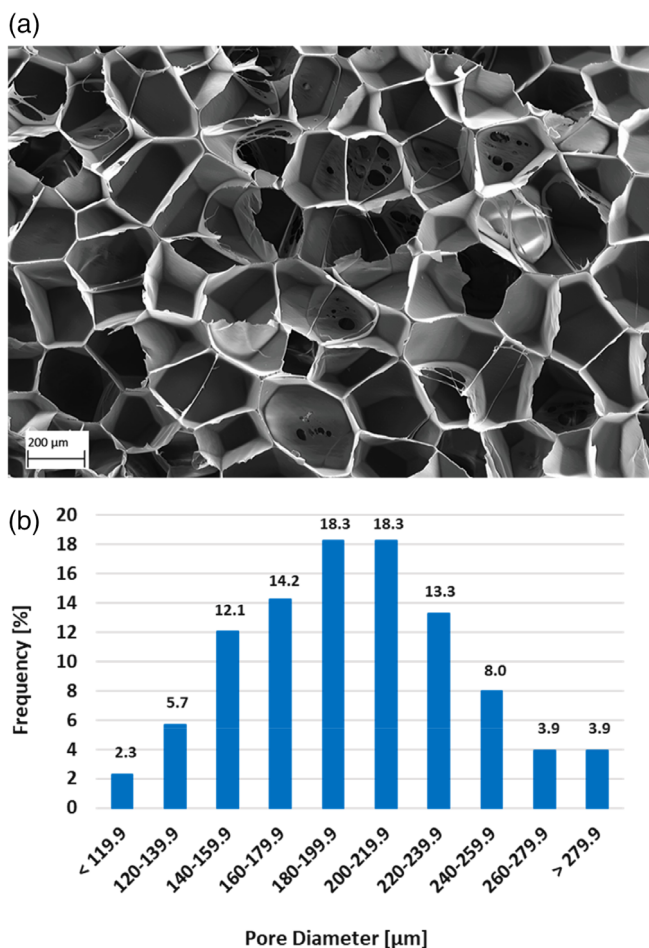| Material property	Value ($\pm$SD)[a]
Density (kg m^{-3})	41.61 ($\pm$0.94)
Expansion ratio	25.24 ($\pm$0.58)
Porosity (%)	96% ($\pm$0)
Open-cell content (%)	90.91 ($\pm$0.21)
Closed-cell content (%)	4.24 ($\pm$0.28)
Cell wall content (%)	4.86 ($\pm$0.11)

[a]$n = 6$.

(a)

(b)

FIGURE 2 (a) Scanning electron microscope micrograph of open-cell polystyrene foam with view width of 2.287 mm and (b) histogram of pore size distribution [Color figure can be viewed at wileyonlinelibrary.com]

the cell wall content (4.86%). The morphology of the cellular PS structure was characterized by the SEM micrographs as shown in Figure 2a. The foam structure primarily exhibited open cells (pores) with irregular shapes. The open cells were interconnected with smaller pores on their cellular walls (Figure 2a). This can provide the porous foam matrix with tortuous paths. Each pore size was determined by diameter of the fitted circle on its perimeter. The pore diameter measurements were performed on two adjacent cross-sections of the foam samples providing a good representation of their pore size distribution. The frequency of the measured pore diameters is presented in a histogram shown in Figure 2b. The reticulated PS foam showed a wide pore size distribution with (93.8%) of the pores with diameters in range of (120–280 μm). However, a substantial portion of the pore diameters (36.6%) was distributed in the narrower range of (180–220 μm). Large pores with diameter (>280 μm) formed (3.9%) with pore diameters reaching (340 μm).

3.2 | Chemical composition of polystyrene foam

The elemental composition of PS foam before and after plasma treatment is illustrated in the XPS survey spectra in Figure 3a,b. The atomic concentrations of the detected surface elements are presented in Table 2. The spectrum of untreated PS showed a distinct C 1 s peak for carbon and small O 1 s peak for oxygen as the major elements of the PS surface. This revealed the predominantly carbon-based composition of pristine PS with C% of 99.49% and O% of 0.47%. The plasma-treated PS spectrum exhibited a very small new peak for nitrogen N 1 s with a more distinct O 1 s peak as shown in Figure 3b. The O_2 plasma treatment introduced more oxygen to the PS surface resulting in a higher relative oxygen concentration of 18.38%, while the carbon concentration decreased to 81.17%. The corresponding Oxygen/Carbon ratio (O/C) of untreated and plasma-treated PS was 0.47% and 22.64% respectively. The nitrogen element was incorporated to the plasma-treated PS accounting for small concentration of 0.32%, and traces of silicon element <0.20% was also found on PS foam surface as presented in Table 2.

The high-resolution C 1 s peak was deconvoluted to its components to identify the bonds and functional groups on the PS surface. Figure 3c,d show the sub-peaks of the deconvoluted C 1 s peak before and after plasma treatment. The analyzed C 1 s peak revealed three peak components for untreated PS defined at binding energy of 284.6, 286.2, and 291.2 eV. This corresponded to bonds of C=C/C—C/C—H, C—O, and π–π* shake-up respectively. The plasma treatment led to emerging new functional groups of C=O, O—C=O, and O—C(=O)—O at binding energies of 287.3, 288.4, and 289.5 eV respectively. The C=C, C—C, C—H bonds were defined at binding energy of 284.6 eV, lower than their normal binding energy (285.0 eV) due to the presence of aromatic rings in the PS structure.[43] The untreated PS showed prevalence of C=C, C—C and C—H bonds with concentration of 92.74% as presented in Table 3. C—O and shake-up bonds were detected with small concentrations of 2.73% and 4.54% respectively. On the other hand, the plasma treatment resulted in a substantial decrease in the C=C, C—C, and C—H bonds to reach 80.56% with increasing concentration of C—O bond to 10.67%. The shake-up (π–π*) bond concentration notably decreased to 0.89% after the plasma treatment and the new polar functional groups of C=O, O—C=O and O—C(=O)—O had small concentrations of 4.38%, 1.57%, and 1.94% respectively.
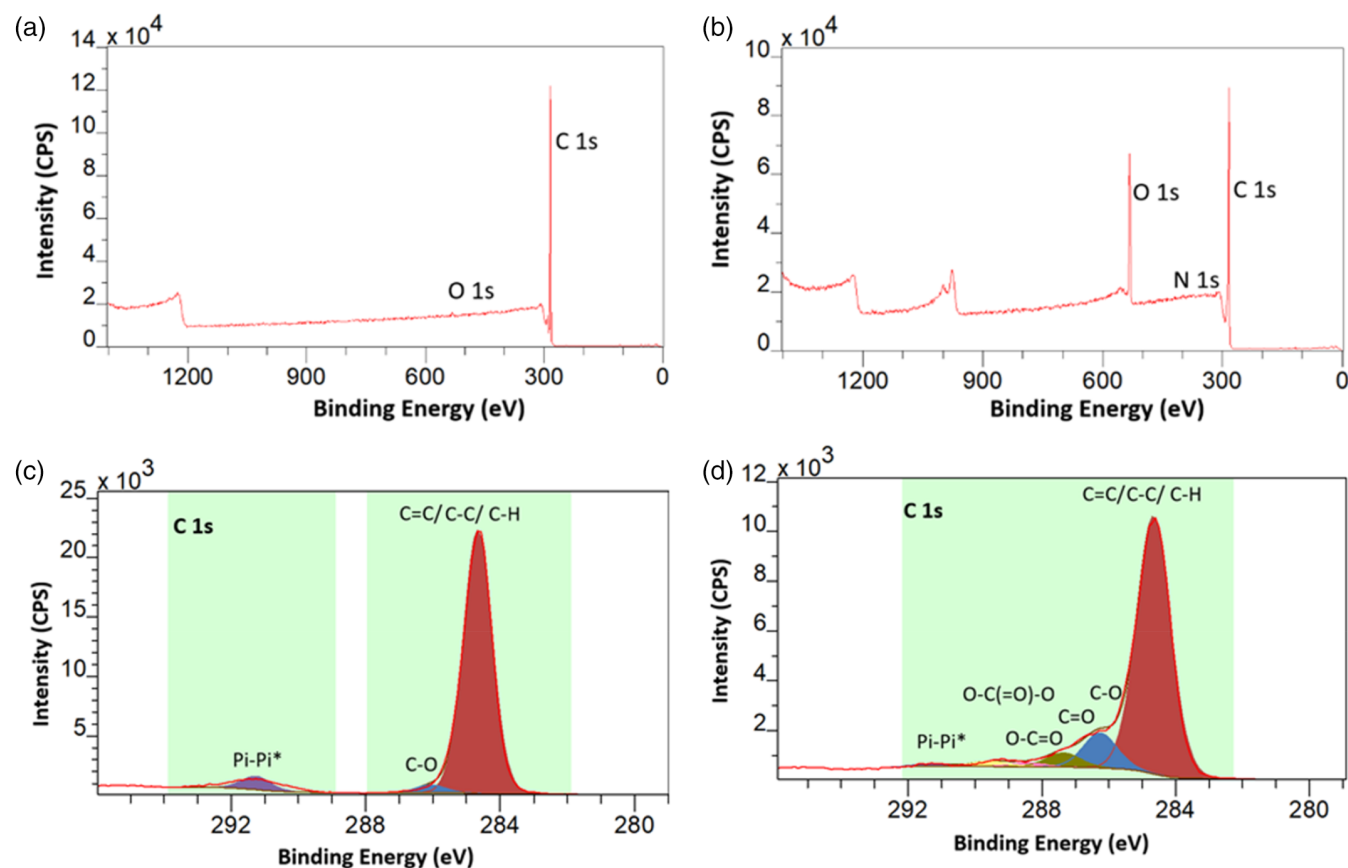
FIGURE 3 Wide X-ray photoelectron spectroscopy spectra of (a) untreated and (b) plasma-treated polystyrene (PS) foam, and functional groups of deconvoluted C 1 s peak for (c) untreated, and (d) plasma-treated PS foam [Color figure can be viewed at wileyonlinelibrary.com]

TABLE 2 Analysis of elemental composition and O/C ratio of polystyrene (PS) foam surface

PS foam surface	C%	O%	N%	O/C[a]
Untreated	99.49	0.47	–	0.47
Plasma-treated for 27 s	81.17	18.38	0.32	22.64

[a]Traces of Si < 0.20%.

3.3 | Surface wettability of polystyrene foam

The surface wettability of PS foam was determined by measuring the apparent contact angle of DI water drops on the foam skin. The measured WCA of PS foam

decreased from $86.01° \pm 0.86°$ for untreated samples to $15.13° \pm 0.70°$ for plasma-treated samples, indicating a substantial increase in surface hydrophilicity. The enhanced surface wettability was also observed in the drop absorption test on the foam cross-section with exposed porous structure. The red-dyed water drops on untreated PS foam showed high contact angle value of $100.15° \pm 4.74°$, while the high-speed camera $(500\,\mathrm{f\,s^{-1}})$ showed instantaneous wicking of water drops into the bulk structure of plasma-treated PS foam within a time of 0.062 ± 0.020 s. This was illustrated in photograph of the instant absorption of water drop on the plasma-treated foam sample in comparison with large water drop on the untreated sample as shown in Figure 4.

TABLE 3 Analysis of C 1 s components of polystyrene foam surface

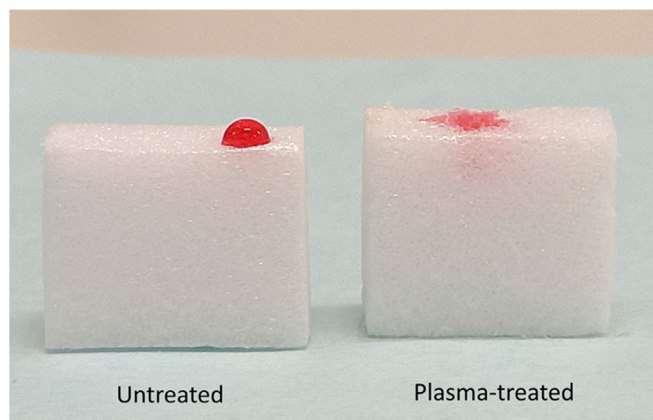| Bond	C=C, C—C, C—H	C—O	C=O	O—C=O	O—C(=O)—O	π–π*
Binding energy (eV)	284.6	286.2	287.3	288.4	289.5	291.2
Untreated	92.74	2.73	–	–	–	4.54
Plasma-treated for 27 s	80.56	10.67	4.38	1.57	1.94	0.89

FIGURE 4 Photograph of red-dyed water drops on untreated and plasma-treated cross-sections of PS foam samples ($L \times W \times T$: 20 mm $\times$ 20 mm $\times$ 5 mm) [Color figure can be viewed at wileyonlinelibrary.com]

3.4 | Liquid absorption capacity

The liquid uptake of PS foam samples was evaluated in terms of their capacity to absorb and retain the test liquids. Figure 5 compares the retention capacity of untreated and plasma-treated PS foam with liquids of different surface tensions. The untreated PS foam exhibited low retention capacity <1.60 g g^{-1} with test liquids of BSA 8 wt% (γ: 52.0 mN m^{-1}), pure water (γ: 72.6 mN m^{-1}), and water with surfactant (γ: 52.3 mN m^{-1}) and for these liquids, the plasma treatment of the foam samples considerably improved their surface wettability and liquid uptake capacity. This resulted in increases in absorption capacity by 4–8 times depending on the liquid. However, in the case of the water with surfactant at the lowest surface tension (31.5 mN m^{-1}), the liquid highly wetted the foam pores resulting in substantial retention capacity of 8.93 $\pm$ 0.32 g g^{-1} even in the absence of plasma treatment. Therefore, the plasma treatment had no additional effect as it is assumed that the sample was fully saturated.

3.5 | Analysis of aging effect of plasma treatment

The hydrophobic recovery of the aged plasma-treated PS foam was studied through the changes in the wettability and surface chemical composition over time. The aging study was carried out for PS foam samples up to 60 days post plasma treatment. Figure S1, illustrates the WCA developed on PS foam skin over different storage periods. The aging rate was relatively high in the first 3 days post treatment, leading to an increase in the WCA from 15.13° to 29.70°. The PS foam then exhibited a slower rate
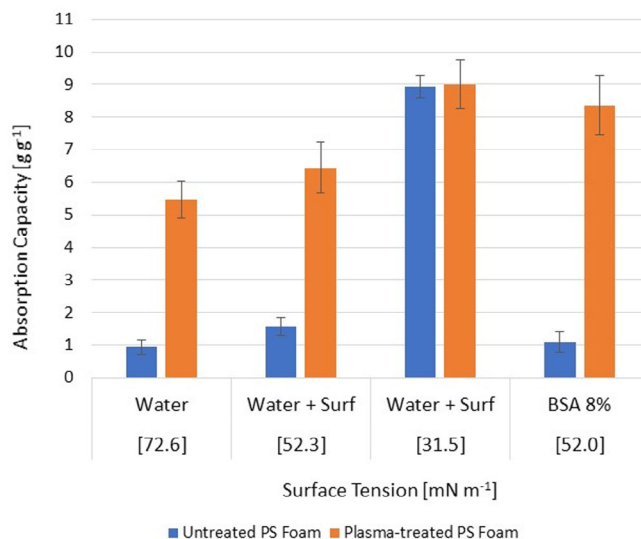

FIGURE 5 Liquid absorption capacity of polystyrene foam with different test liquids [Color figure can be viewed at wileyonlinelibrary.com]
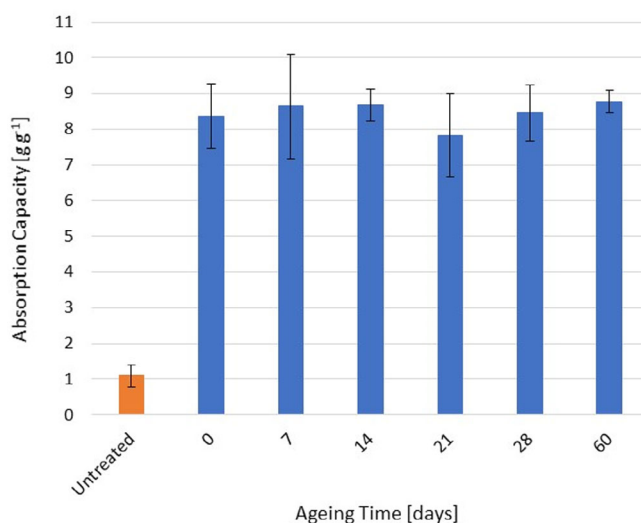

FIGURE 6 Absorption capacity of plasma-treated polystyrene foam with bovine serum albumin 8wt% (γ: 52.0 mN m^{-1}) over different aging times [Color figure can be viewed at wileyonlinelibrary.com]

of aging with a small increase in the WCA showing stable wettability after 28 days of the storage time. This corresponded to WCA of 41.55°, which is still considerably lower than WCA of 86.01° for untreated PS. The chemical composition of the aged PS foam samples also changed with a considerable decrease in the oxygen concentration and O/C ratio, particularly in the first day as shown in Table S1. This corresponded to a drop in O% and O/C ratio from 18.38% and 22.64% respectively at day 0%−15.63% and 18.68% respectively at day 1. However,

the oxygen concentration after 60 days remained relatively high at 13.12% in comparison with O% of 0.47% for the untreated PS samples. The nitrogen concentration was almost unchanged during the storage times. The effect of aging on liquid absorption capacity of the PS foam was assessed during these same aging times. Figure 6 shows the absorption capacity with BSA 8wt% (γ: 52.0 mN m^{-1}) before and after the plasma treatment for storage periods of 0, 7, 14, 21, 28, and 60 days. The PS foam samples had a nearly constant enhanced liquid capacity of about eight times that of the untreated samples, with no deterioration during the 60 days of aging. For practicality of using PS foam as a liquid absorber, the liquid absorption capacity was also normalized in terms of kilograms (liquid) absorbed per cubic meter (foam). This revealed an estimated increase in the absorption capacity of PS foam sheet (nominal thickness: 5 mm) from 45.35 ± 6.53 kg m^{-3} before plasma treatment to 365.34 ± 19.80 kg m^{-3} after 60 days of the O$_2$ plasma treatment.

4 | DISCUSSION

Liquid absorption and retention properties of a porous media, such as PS foam fundamentally depend on both its structural and wetting characteristics.[48] The high porosity and open-cell content of the PS foam are among the crucial structural parameters, which determine the potential for the foam samples to uptake significant liquid quantities. This was reflected in the large gaseous space within the foam matrix as the porosity represents the volume of gaseous cells to the sample volume.[19] The formation of larger cells and thinner cellular membranes can be attributed to the low foam density.[49] A previous work reported an increase in water absorption capacity of polyurethane foam from 0.6 to 6.8 vol% due to a decrease in the foam density from 116 to 42 kg m^{-3}, respectively.[50] The high interconnectivity of the gaseous voids (open cells) also increased the gaseous space available to be filled by absorbed liquids, while the isolated and closed cells had no contribution to the liquid absorption capacity.[50] Others found a strong relationship between the improved liquid absorption capacities of polyurethane foam with an increase in the pore connectivity.[48] Regardless of these attributes, pore surface wettability is a crucial enabler for liquid penetration into PS foam voids under a capillary pressure generated on the foam pores and is key for exploiting the open space in the foam. This pressure is determined by the liquid surface tension, size and wettability of pores as described by Young–Laplace law in the Equation (1). Accordingly, smaller pores with higher hydrophilic surface absorbed the wetting liquid before larger pores due to their higher negative capillary pressure.[22,48,51] The corresponding capillary forces are based on the discrepancy of surface energy on the wet and dry pore surfaces as the wicking liquid tends to wet the pore surfaces.[20,21]

The hydrophobicity and low surface energy of PS foam restrict the interactions between the pore surfaces and water-based fluids.[24] This prevents the liquid penetration into the foam pores as demonstrated in the low absorption capacity of untreated PS foam samples. Thus, the PS foam efficiency as a soak-away is currently limited for food packaging despite the large pore volume. However, the pore surfaces of PS foam had higher hydrophilicity and surface energy after the oxygen plasma treatment.[45] The plasma treatment decreased the WCA on PS foam skin and led to rapid wicking of water into the foam porous structure. The improved foam hydrophilicity allowed the liquid to wet the foam pores and increased their capillary pressure. This resulted in a substantial increase in the liquid wicking and absorption capacity,[22,24,48] and plasma-treated PS foam with BSA 8wt% had an absorption capacity around eight times that of the untreated foam. The pore surfaces were modified through diffusion of the excited gaseous species of plasma into the foam porous structure. This was manifested in activation of the interconnected pores and implanting polar functional groups on their surfaces.[42,52] On the other hand, the plasma treatment had no effect on the absorption capacity of PS foam with water of low surface tension (γ: 31.5 mN m^{-1}). This is due to the already high wetting affinity of the liquid to wet the pore surfaces facilitating the liquid penetration into the foam porous structure.[22] However, liquids with such low surface tensions are not typical of meat exudate.[53] This effect could be analogous to the use of chemical surfactants in the foam as a means of reducing the exudate surface tension.

The O$_2$ plasma treatment improved the hydrophilicity of the PS foam pores by increasing the oxygen content on the treated surfaces.[44] This corresponded to an increase in O/C from 0.47% to 22.64% for untreated and plasma-treated PS foam samples respectively. These results are in line with published research, with different studies reporting comparable improvements in surface hydrophilicity and oxygen contents of plasma-treated PS.[44,54,55] The exposure to the excited plasma species induces hydrogen abstraction and chain scission of PS structure with the primary target being the aromatic rings.[56] This results in formation of reactive radical sites on the treated PS surface.[57] The reaction between these sites and excited oxygen molecules in the plasma glow led to the introduction of different polar oxygen groups including C—OH, C=O, COOH and O—C(=O)—O, which contributed to the decrease in WCA to 15.13°.[44,54] These functional

groups have been reported in previous studies on plasma-treated PS material.[44,55,58] The presence of aromatic rings in the PS structure accounted for the satellite $\pi-\pi^*$ peak. The C 1 s spectrum after the plasma treatment revealed a decrease in $\pi-\pi^*$ peak intensity, which can be ascribed to a targeting of the C=C bonds within the aromatic rings. This may have resulted in opening the rings and generating new polar oxygen groups, such as the carbonate group O—C(=O)—O and carboxyl group (O=C—OH) as described by other studies.[44,58] The plasma-treated PS can remain reactive due to unreacted radical sites, and the presence of a small nitrogen peak may originate from the post-treatment reaction between the atmospheric air and available radical sites. The presence of small amounts of other elements on the PS structure is assumed to originate from the PS oxidation in the case of oxygen and contamination in the case of silicon.[43,59]

Polymeric materials functionalized with oxygen plasma experience hydrophobic recovery because of aging. This corresponds to a decay of polar oxygen groups and a tendency of the polymer surface to lose some of the gained hydrophilicity.[44] The plasma-treated PS foam showed reduction in the surface wettability with an increase in the WCA over time. Previous studies on aged PS after plasma treatments showed similar tendency of PS surface to become more hydrophobic with decreases in surface oxygen content during aging time.[43,44,55] Although WCA increased to 41.90° after 60 days, it remained significantly lower than WCA of 86.01° for untreated PS foam. This was consistent with the decrease in O% and O/C ratios over the same storage time. The aging effect can occur due to reorientation of the PS polymer chains leading to burying of the oxygen groups into the polymer matrix. The formation of hydroperoxides on the treated PS surface can also facilitate the aging process. These hydroperoxide products are instable leading to decay in the surface polarity and hydrophilicity. However, the aging process resulted only in a partial loss of the surface wettability and oxygen concentration. Therefore, the plasma treatment induced a permanent increase in the foam wettability.[44] The maintained improvement in the foam wettability allowed liquids, even with high surface tensions, to wet the foam pores. The corresponding negative capillary pressures acting on the pores provided the PS foam with liquid sucking functionality. This was evident with a maintained high absorption capacity of aged PS foam with BSA 8wt% at more than eight times that of untreated PS foam. Thus, it is viable to fully treat the PS foam with plasma whether in the form of a finished absorbent food tray or sheet. This can be achieved through perforation of the foam skin to allow the excited plasma species to penetrate the internal foam pores.

5 | CONCLUSION

In this work, oxygen plasma treatment of open-cell PS foam revealed improvement in wettability of the foam porous structure. The exposure of the porous structure of PS foam to the plasma introduced polar oxygen groups onto the pore surfaces and improved their wettability. This increased the capillary pressure acting on the pores allowing larger liquid uptake and absorption. The plasma-treated foam samples had a substantial and durable increase in their liquid absorption capacity (g g^{-1}) of eight times higher than the pristine foam samples. Therefore, one cubic meter of the PS foam sheet gained liquid absorption capacity of about 365 kg after plasma treatment in comparison with only about 45 kg for untreated PS foam. The wettability increases experienced partial loss due to the decrease in the oxygen groups under the effects of the aging phenomenon. However, the aged foam pores maintained surface wettability distinctly higher than the untreated foam pores after 60 days post plasma treatment. This was sufficient for the liquids to wet the pore surfaces inducing instant liquid wicking and absorption, with no drop in performance over time. This showed the efficiency and practicality of using plasma technology for improving liquid scavenging within food packaging. This ensures higher absorption capacity and rapid wicking of any excessive food liquid, and thus, helps take the exuded liquid away from the packaged food. The open-cell polymeric foams can be used as soak-away for meat exudate or other food juices in form of whole packaging trays (acting as both package and soak-away) or absorbent pad without the need for chemical wetting agents. The surface treatment of foam materials can be continuous and economical through integration of an atmospheric plasma unit into current packaging production lines.

CONFLICT OF INTEREST
The authors declare no conflict of interest.

DATA AVAILABILITY STATEMENT

The data that support the findings of this study are available from the corresponding author upon reasonable request.

ORCID

Alaa Alaizoki https://orcid.org/0000-0003-2208-4295
Christopher Phillips https://orcid.org/0000-0001-8011-710X
James McGettrick https://orcid.org/0000-0002-7719-2958
Davide Deganello https://orcid.org/0000-0001-8341-4177

REFERENCES

[1] K. K. Gaikwad, S. Singh, A. Ajji, *Environ. Chem. Lett.* **2019**, *17*, 609.

[2] K. T. Lee, *Meat Sci.* **2010**, *86*, 138.

[3] B. Schumann, M. Schmid, *Innov. Food Sci. Emerg. Technol.* **2018**, *47*, 88.

[4] M. B. Cole, M. A. Augustin, M. J. Robertson, J. M. Manners, *npj Sci. Food* **2018**, *2*, 14.

[5] FAO, Global Food Losses and Food Waste—Extent, Causes and Prevention, Technical Report **2011**.

[6] I. Ahmed, H. Lin, L. Zou, A. L. Brody, Z. Li, I. M. Qazi, T. R. Pavase, L. Lv, *Food Control* **2017**, *82*, 163.

[7] G. D. Kim, E. Y. Jung, H. J. Lim, H. S. Yang, S. T. Joo, J. Y. Jeong, *Meat Sci.* **2013**, *95*, 323.

[8] E. Huff-Lonergan, S. M. Lonergan, *Meat Sci.* **2005**, *71*, 194.

[9] R. D. Warner, *Lawrie's Meat Science*, 8th ed., Woodhead Publishing Limited, Cambridge **2017**, p. 419.

[10] L. A. Van Rooyen, P. Allen, D. I. O'Connor, *Meat Sci.* **2017**, *132*, 179.

[11] D. M. Gouvêa, R. C. S. Mendonça, M. E. S. Lopez, L. S. Batalha, *LWT- Food Sci. Technol.* **2016**, *67*, 159.

[12] C. E. Realini, B. Marcos, *Meat Sci.* **2014**, *98*, 404.

[13] R. P. Davidson, G. S. Becke, J. C. Minnett, Food Tray with Integrated Liquid-Retention System. United States patent US8596490. **2013**

[14] J. M. LaRue, C. E. Cappel, F. A. Petlak, Container Having Internal Reservoir, United States patent US7921992. **2010**

[15] C. G. Otoni, P. J. P. Espitia, R. J. Avena-Bustillos, T. H. McHugh, *Food Res. Int.* **2016**, *83*, 60.

[16] D. G. Bland, W. G. Stobby, G. D. Rose, S. W. Mork, T. L. Staples, G. D. McCann, Absorbent, Extruded Thermoplastic Foams, United States patent US006071580. **2000**

[17] E. A. Colombo, J. J. Braddon, Food Package with Integral Juice Absorbing Bottom, United States patent US6695138. **2004**

[18] S. Gunashekar, K. M. Pillai, B. C. Church, N. H. Abu-Zahra, *J. Porous. Mater.* **2015**, *22*, 749.

[19] J. Pinto, A. Athanassiou, D. Fragouli, *J. Environ. Manag.* **2018**, *206*, 872.

[20] R. Masoodi, K. M. Pillai, *J. Porous Media* **2012**, *15*, 775.

[21] R. Masoodi, H. Tan, K. M. Pillai, *AICHE J.* **2011**, *57*, 1132.

[22] E. Unsal, J. H. Dane, P. Schwartz, *J. Appl. Polym. Sci.* **2005**, *97*, 282.

[23] J. Hou, G. Zhao, L. Zhang, G. Wang, B. Li, *J. Colloid Interface Sci.* **2019**, *542*, 233.

[24] L. Safinia, K. Wilson, A. Mantalaris, A. Bismarck, *Macromol. Biosci.* **2007**, *7*, 315.

[25] L. Zanderighi, *Packag. Technol. Sci.* **2001**, *14*, 267.

[26] J. J. Krueger, F. R. Radwanski, M. G. Reichmann, P. R. Elliker, A. Yahiaoui, R. E. Richard, O. P. Thomas, Low-density, open-cell, soft, flexible, thermoplastic, absorbent foam and method of making foam, Google Patents, US7358282. **2008**

[27] P. T. Dirlam, D. J. Goldfeld, D. C. Dykes, M. A. Hillmyer, *ACS Sustainable Chem. Eng.* **2019**, *7*, 1698.

[28] C. Cowan-Ellsberry, S. Belanger, P. Dorn, S. Dyer, D. McAvoy, H. Sanderson, D. Versteeg, D. Ferrer, K. Stanton, C. Cowan-ellsberry, D. Mcavoy, *Crit. Rev. Environ. Sci. Technol.* **1893**, *2014*, 44.

[29] S. Rebello, A. K. Asok, S. Mundayoor, M. S. Jisha, *Environ. Chem. Lett.* **2014**, *12*, 275.

[30] P. Fabbri, M. Messori, *Modification of Polymer Properties*, Elsevier Inc, Oxford **2017**, p. 109.

[31] N. Vandencasteele, F. Reniers, *J. Electron Spectros. Relat. Phenom.* **2010**, *394*, 178.

[32] A. Vesel, M. Mozetic, *J. Phys. D. Appl. Phys.* **2017**, *50*, 21.

[33] K. T. Lee, J. M. Goddard, J. H. Hotchkiss, *Packag. Technol. Sci.* **2009**, *22*, 139.

[34] M. Ozdemir, C. U. Yurteri, H. Sadikoglu, *Crit. Rev. Food Sci. Nutr.* **1999**, *39*, 457.

[35] M. J. Shenton, G. C. Stevens, *J. Phys. D. Appl. Phys.* **2001**, *34*, 2761.

[36] A. Van Deynse, P. Cools, C. Leys, N. De Geyter, R. Morent, *Appl. Surf. Sci.* **2015**, *328*, 269.

[37] S. Canbolat, M. Kilinc, D. Kut, *Procedia. Soc. Behav. Sci.* **2015**, *195*, 2143.

[38] C. W. Kan, Y. L. Lam, *Fibers Polym* **2015**, *16*, 1705.

[39] R. López, M. Pascual, D. García-Sanoguera, L. Sánchez-Nacher, R. Balart, *Fibers Polym.* **2012**, *13*, 1139.

[40] A. Alaizoki, C. Phillips, D. Parker, C. Hardwick, C. Griffiths, D. Deganello, *Food Packag. Shelf Life* **2021**, *30*, 100759.

[41] E. Laguna-Gutierrez, R. Van Hooghten, P. Moldenaers, M. A. Rodriguez-Perez, *J. Appl. Polym. Sci.* **2015**, *132*, 42430.

[42] L. Sahnia, K. Wilson, A. Mantalaris, A. Bismarck, *J. Biomed. Mater. Res. - Part A* **2008**, *87*, 632.

[43] O. M. Ba, P. Marmey, K. Anselme, A. C. Duncan, A. Ponche, *Colloids Surf. B Biointerfaces* **2016**, *145*, 1.

[44] A. Vesel, *Surf. Coat. Technol.* **2010**, *205*, 490.

[45] C. Canal, F. Gaboriau, A. Vílchez, P. Erra, M. J. Garcia-Celma, J. Esquena, *Plasma Process. Polym.* **2009**, *6*, 686.

[46] A. Rizvi, R. K. M. Chu, J. H. Lee, C. B. Park, *ACS Appl. Mater. Interfaces* **2014**, *6*, 21131.

[47] Y. Yao, M. Yoshioka, N. Shiraishi, *J. Appl. Polym. Sci.* **1939**, *1996*, 60.

[48] J. Pinto, A. Athanassiou, D. Fragouli, *J. Phys. D. Appl. Phys.* **2016**, *49*, 145601.

[49] H. T. T. Duong, R. P. Burford, *J. Appl. Polym. Sci.* **2006**, *99*, 360.

[50] M. Thirumal, D. Khastgir, N. K. Singha, B. S. Manjunath, Y. P. Naik, *J. Appl. Polym. Sci.* **1810**, *2008*, 108.

[51] S. Ravi, R. Dharmarajan, S. Moghaddam, *Langmuir* **2015**, *31*, 12954.

[52] L. Safinia, N. Datan, M. Höhse, A. Mantalaris, A. Bismarck, *Biomaterials* **2005**, *26*, 7537.

[53] A. V. Ursu, A. Marcati, P. Michaud, G. Djelveh, *J. Food Eng.* **2016**, *190*, 54.

[54] C. C. Dupont-Gillain, Y. Adriaensen, S. Derclaye, P. G. Rouxhet, *Langmuir* **2000**, *16*, 8194.

[55] M. Häidopoulos, M. Horgnies, F. Mirabella, J. J. Pireaux, *Plasma Process. Polym.* **2008**, *5*, 67.

[56] J. Davies, C. S. Nunnerley, A. C. Brisley, R. F. Sunderland, J. C. Edwards, P. Krüger, R. Knes, A. J. Paul, S. Hibbert, *Colloids Surfaces A Physicochem. Eng. Asp.* **2000**, *174*, 287.

[57] M. Dhayal, M. R. Alexander, J. W. Bradley, *Appl. Surf. Sci.* **2006**, *252*, 7957.

[58] A. Vesel, R. Zaplotnik, J. Kovac, M. Mozetic, *Plasma Sources Sci. Technol.* **2018**, *27*, 094005.

[59] K. Fricke, H. Tresp, R. Bussiahn, K. Schröder, T. Von Woedtke, K. D. Weltmann, *Plasma Chem. Plasma Process.* **2012**, *32*, 801.

SUPPORTING INFORMATION

Additional supporting information may be found in the online version of the article at the publisher's website.